On the O_2 Binding of Fe–Porphyrin, Fe–Porphycene, and Fe–Corrphycene Complexes

HIROYUKI NAKASHIMA, JUN-YA HASEGAWA, HIROSHI NAKATSUJI
Department of Synthetic Chemistry and Biological Chemistry, Graduate School of Engineering, Kyoto University, Katsura, Nishikyo-ku, Kyoto 615-8510, Japan

Received 7 December 2005; Accepted 25 February 2006
DOI 10.1002/jcc.20447
Published online in Wiley InterScience (www.interscience.wiley.com).

Abstract: Based on our previous study for the O_2 binding of the Fe–Por complex, this study investigates the O_2 binding mechanism in the Fe–porphyrin isomers, Fe–porphycene (FePc), and Fe–corrphycene (FeCor) complexes. By calculating the potential energy surface of the O_2 binding, the present study explains the reason for the dramatic increase of O_2 affinities observed in the FePc complex. In the case of FeCor–O_2, the O_2 binding process includes the intersystem crossing from a triplet to singlet state, as in the FePor–O_2 complex. However, FePc–O_2 uses only a singlet surface. This is because the ground state of the FePc complex in the deoxy state is a triplet state, while those of FePor and FeCor are a quintet state. Such difference originates from character of the SOMO. We estimated an equilibrium constant for the O_2 binding that reasonably reproduced the trend observed in the experiments.

 J Comput Chem 27: 1363–1372, 2006

Key words: O_2 binding; heme; porphycene; corrphycene; potential energy surface

Introduction

Hemoglobin and myoglobin play important roles in our daily life through the transport and storage of O_2. These processes have been studied in detail both theoretically and experimentally.[1–27] Hemoglobin and myoglobin are well-known heme proteins. They are also useful for engineering applications.[28–43] To understand and control their functions, myoglobin has been subjected to extensive modifications. They are classified into two categories: amino acid mutation,[28–32] and the replacement of the protoporphyrin by artificial porphyrin isomers.[33–43] The former approach is mainly suitable for regulating delicate physiological reactions. In contrast, the latter approach is expected either to improve its functions or to introduce new functions, because the active center itself is replaced by another one. Several modified myoglobins have been experimentally realized using the latter approach. For example, the protoporphyrin has been replaced by aza-porphyrin, diaza-porphyrin, tetra-aza porphyrin, porphycene, corrphycene, etc.[33–39]

Among the interesting properties that the reconstituted myoglobins exhibit, we particularly focused on the O_2 binding property. Hayashi et al.[36,37] reported that the replacement of porphyrin by porphycene in myoglobin had extremely high O_2 affinity, which is by more than 1000 times higher than that of the native myoglobin. This finding indicates a possibility to realize tailor-made functional protein.[37] In contrast, Neya et al.[38,39] reported that the replacement by corrphycene lowered the O_2 affinity (about 1/100 times). These dramatic changes were introduced only by the substitution of the porphyrin ring. Porphycene[36,37] and corrphycene[38,39] are porphyrin isomers that have (2,0,2,0) and (2,1,0,1) carbon atoms between each pyrrole rings, respectively, as shown in Figure 1. These isomers interact to the Fe atom in different ways, and the electronic structures could be unique among the reconstituted heme. In this case, a theoretical study would provide important information about the electronic structure basis to understand the O_2 affinity. It would be difficult by anything other than by the experimental studies to conclude which factor controls the O_2 binding properties.

Several theoretical studies have been performed for the O_2, CO, and NO bindings to the heme and their derivatives at several theoretical levels, MNDO/d,[15] QM/MM,[16–18] DFT with LSD schemes,[19–21] CASSCF,[22–24] CASPT2,[25] and SAC/SAC-

Correspondence to: H. Nakatsuji; e-mail: hiroshi@sbchem.kyoto-u.ac.jp

Contract/grant sponsor: The Grant for Creative Scientific Research from the Ministry of Education, Science, Sports and Culture

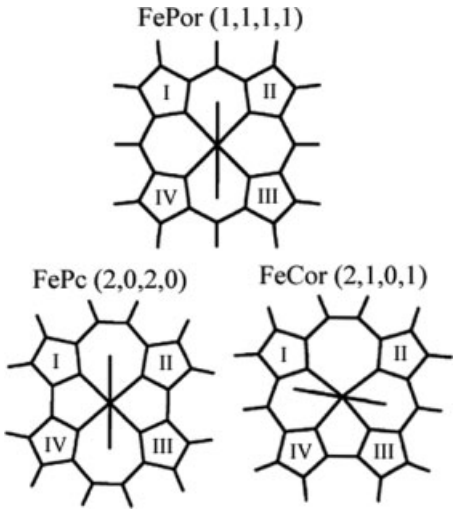

Figure 1. Structures of Fe–porphyrin (FePor), Fe–porphycene (FePc), and Fe–corrphycene (FeCor) complexes. Porphyrin has (1,1,1,1) carbons, porphycene has (2,0,2,0) carbons, and corrphycene has (2,1,0,1) carbons between pyrrole rings. The numbers in the parenthesis, ($n_{I–II}$, $n_{II–III}$, $n_{III–IV}$, $n_{IV–I}$) are number of the carbon atoms between the pyrrole rings. The "$n_{I–II,}$" "$n_{II–III,}$" "$n_{III–IV,}$" and "$n_{IV–I}$" denotes the number of the carbon atoms between the rings I and II, II and III, III and IV, and IV and I, respectively.

CI[26] calculations. Recently, many DFT calculations were also performed, and the electronic structures of ligand-binding complexes or the effects of the proximal and distal sites in the protein environment were investigated.[9–14] In the present study, we are interested in the O_2 binding process to the heme and its isomers of proto-porphyrin. We discuss here the electronic structures of the O_2 binding complexes, comparing our calculations with several other theoretical studies.

In our previous study,[44] we investigated the electronic mechanism of the reversible O_2 binding by heme (FePor). For the O_2 binding process, we found that the spin state was primarily important. Out-of-plane deviation of the Fe atom from the porphyrin plane was also an important factor. Our conclusion for oxyheme is as follows. (1) The potential energy surface of the lowest singlet state is associative, while that of the lowest triplet state is dissociative. (2) The Fe atom locates in-plane in the singlet state, while it is out-of-plane in the triplet state. (3) The O_2 binding process obviously include intersystem crossing from triplet to singlet states. (4) This crossing requires relativistic spin-orbit interaction. (5) Owing to such intersystem crossing, the activation energies for both O_2 binding and dissociation become moderate, and hence, reversible. (6) The electronic structure of the ground state of the oxyheme would be an open singlet state.

In this study, we have extended our previous study to the Fe–porphycene–Imidazole (FePc) and Fe–corrphycene–Imidazole (FeCor) isomers and clarified the potential surface of the O_2 binding processes. Based on these calculations, a reasonable explanation has been given to the previous experimental results. As seen later, the electronic and molecular structures of the deoxy-states and oxy-states are discussed, respectively. Then the potential energy surface and the O_2 binding processes are discussed, and we estimated the equilibrium constant for the O_2 binding, and the result was compared with the experimental data.

Computational Details

DFT (UB3LYP) calculations were performed with the Gaussian98 program package.[45] The heme model used in this study is O_2–Fe–X–Imidazole complex.[44] For FePor, FePc, and FeCor, "X" is porphin, porphycene, and corrphycene, respectively. In myoglobin and its analogs, where the protoporphyrin of heme was replaced with the artificial porphyrin isomers (Pc and Cor), the electronic structure of the Fe atom is a ferrous state (Fe(II)) in the O_2 dissociation limit.[33–43] So, we calculated the ferrous states for deoxy complexes and the O_2 binding states with the same number of electrons. As described in a later section, the electronic structure of the O_2 binding state is close to the ferric state (Fe(III)), Fe(III)+ O_2^-. The basis sets for the Fe, O, and pyrrole N atoms were 6-31g* set.[46] The rest of atoms are treated by 6-31g set for the other atoms.[46] Solomon et al. did some extensive tests of the functional and basis set dependence for the O_2 and NO bindings to the nonheme complexes.[11] But, because we wanted to compare the results of the present isomers with the results of heme in our previous article, we used the same basis set and methodology.[44]

To determine the electronic structure of the ground states, we performed the geometry optimizations for deoxy complexes in singlet, triplet, and quintet states and oxy complexes in singlet and triplet states. As shown in a later section, the ground state of the O_2 binding state has open-shell singlet nature. This state was calculated by using the guess of the triplet state having the same electronic configuration in the SCF step.

Then, we calculated the two-dimensional potential energy surfaces of the O_2 binding process in the singlet and triplet states. The reaction coordinates are (1) the deviation of the Fe atom from the ring plane, and (2) the distance between Fe and O_2. These two reaction coordinates are referred as d and R, respectively. See Figure 2 for the graphical representations. We calculated 46, 38, and 46 points on the potential surface for FePor, FePc. and FeCor, respectively. The intervals are 0.1 and

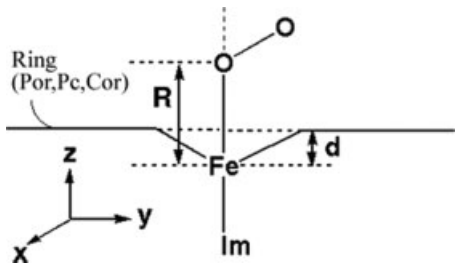

Figure 2. The computational model and the two reaction coordinates, d (the deviation of the Fe atom from the ring plane) and R (the distance between Fe and O_2). The "Im," "Por," "Pc," and "Cor" denote imidazole, porphyrin, porphycene, and corrphycene rings, respectively.

Table 1. The Optimized Geometries and Total Energies of the Deoxy Complexes in Quintet, Triplet, and Singlet State.

	FcPor			FePc			FcCor		
	Quintet	Triplet	Singlet	Quintet	Triplet	Singlet	Quintet	Triplet	Singlet
Relative energy (kcal/mol)	**0.00**	**0.671**	**6.48**	**4.70**	**0.00**	**9.97**	**0.00**	**3.59**	**12.6**
				Optimized geometry					
Distance (Å)									
Fe–Im N	2.13	2.21	1.91	2.12	2.21	1.92	2.12	2.19	1.92
Fe–Pyr N_I	2.09	2.01	2.01	1.95	1.95	1.95	2.09	2.06	2.05
Fe–Pyr N_{II}	2.09	2.01	2.02	1.95	1.95	1.95	2.10	2.07	2.05
Fe–Pyr N_{III}	2.09	2.01	2.01	1.95	1.95	1.95	2.10	1.95	1.96
Fe–Pyr N_{IV}	2.09	2.01	2.01	1.95	1.95	1.95	2.10	1.95	1.96
Fe–ring plane	**0.429**	**0.190**	**0.201**	**0.260**	**0.231**	**0.233**	**0.513**	**0.213**	**0.224**
Angle (degree)									
Pyr N_I–Fe–Pyr N_{II}	88.8	89.1	89.7	94.2	96.2	96.1	107.6	102.7	103.4
Pyr N_{II}–Fe–Pyr N_{III}	88.7	90.4	89.6	84.1	82.9	83.1	85.0	88.5	88.3
Pyr N_{III}–Fe–Pyr N_{IV}	88.6	89.0	89.6	94.4	96.2	96.1	74.2	78.6	78.5
Pyr N_{IV}–Fe–Pyr N_I	88.7	90.4	89.7	84.1	82.9	83.1	85.6	88.7	88.3
Pyr N_I–Fe–Im N	98.6	94.2	95.2	96.3	94.5	94.6	100.9	95.7	95.1
Pyr N_{II}–Fe–Im N	99.9	94.2	94.2	96.4	94.5	94.5	98.0	94.7	94.5
Pyr N_{III}–Fe–Im N	96.6	93.9	94.6	97.3	95.5	95.1	102.3	93.5	94.0
Pyr N_{IV}–Fe–Im N	99.9	93.9	94.2	97.4	95.4	95.1	101.1	94.9	94.4
Dihedral angle (degree)									
Pyr N_I–Fe–Im N–Im C	90.4	135.4	135.0	46.5	46.8	46.9	105.8	149.7	142.6
Pyr N_{II}–Fe–Im N–Im C	0.204	44.7	45.0	−48.5	−49.8	−49.6	−4.01	46.4	38.6
Pyr N_{III}–Fe–Im N–Im C	−90.1	−44.5	−44.9	−133.3	−133.1	−133.1	−90.6	−42.4	−50.0
Pyr N_{IV}–Fe–Im N–Im C	−179.9	−135.2	−135.0	131.3	130.1	130.3	−166.7	−121.2	−128.7

The total energy of ground state is taken as 0.00 kcal/mol.

0.2 Å for the coordinates d and R, respectively. For the R, a finer grid of 0.1 Å interval was taken near minimal point. In this calculation, other atomic coordinates except for d and R were changed linearly between the optimized geometry for the O_2 binding states and that for O_2 dissociation limit. We first optimized the atomic coordinates for O_2 binding state (X_{bind}) and O_2 dissociation limit (X_{dis}). With a parameter λ ($0 < \lambda \leq 1$), the atomic coordinates between the two structures were linearly defined as eq. (1).

$$\mathrm{X} = \lambda \mathrm{X}_{bind} + (1 - \lambda)\mathrm{X}_{dis}. \quad (1)$$

At each point, the Fe–O_2 distance, R, was changed keeping all other geometric parameters fixed. The structural parameters except for R and d were linearly changed between the O_2 binding state and the dissociation limit: in this limited approximation, the relaxation effects are contained in our calculations. In our previous article for the FePor case, we examined the full relaxation effects of the potential energy surfaces by the geometry optimization with fixed R and d, and the energy change due to the relaxation was calculated to be less than 1.08 kcal/mol on the singlet surface of the intermediate region between the O_2 binding state and the dissociation limit.[44] This region was expected to be largest deviating in the examined process. So, the error in the potential surfaces due to the lack of the full structural relaxation was expected to be at most 1 kcal/mol. We thought this would hold also for the present systems.

Results and Discussion

Ground States of the Deoxy Complexes: Electronic Structure and Geometry

The spin-multiplicity and the geometry of the deoxy complexes were determined by the geometry optimization in each spin multiplicity. Table1 shows some important structural parameters and relative energies of the complexes.

The ground state of FePor was calculated to be a quintet state.[44] The triplet and singlet states are located 0.67 and 6.48 kcal/mol higher than the quintet state, respectively. The optimized geometry of the quintet state was quite different from those of the triplet and singlet states. In the quintet state, the deviation of the Fe atom from the ring plane was 0.421 Å, which was much larger than the case of the triplet (0.190 Å) and the singlet states (0.201 Å). The calculated geometry for the quintet state is in good agreement with the experimental X-ray crystallographic data[44] for myoglobin and a biomimetic complexes.[47–51] In the present calculations, the energy gap between the quintet and triplet state is so small (0.67 kcal/mol) that so we cannot justify the quintet state being the ground state from only the present theoretical result. However, fortunately, these experimental findings seem to support that the ground state may be the quintet state.[47–51]

For FeCor, the ground state was also a quintet state as in FePor. The energy gaps between the quintet state and the other states were, however, larger than the case of FePor. The Fe

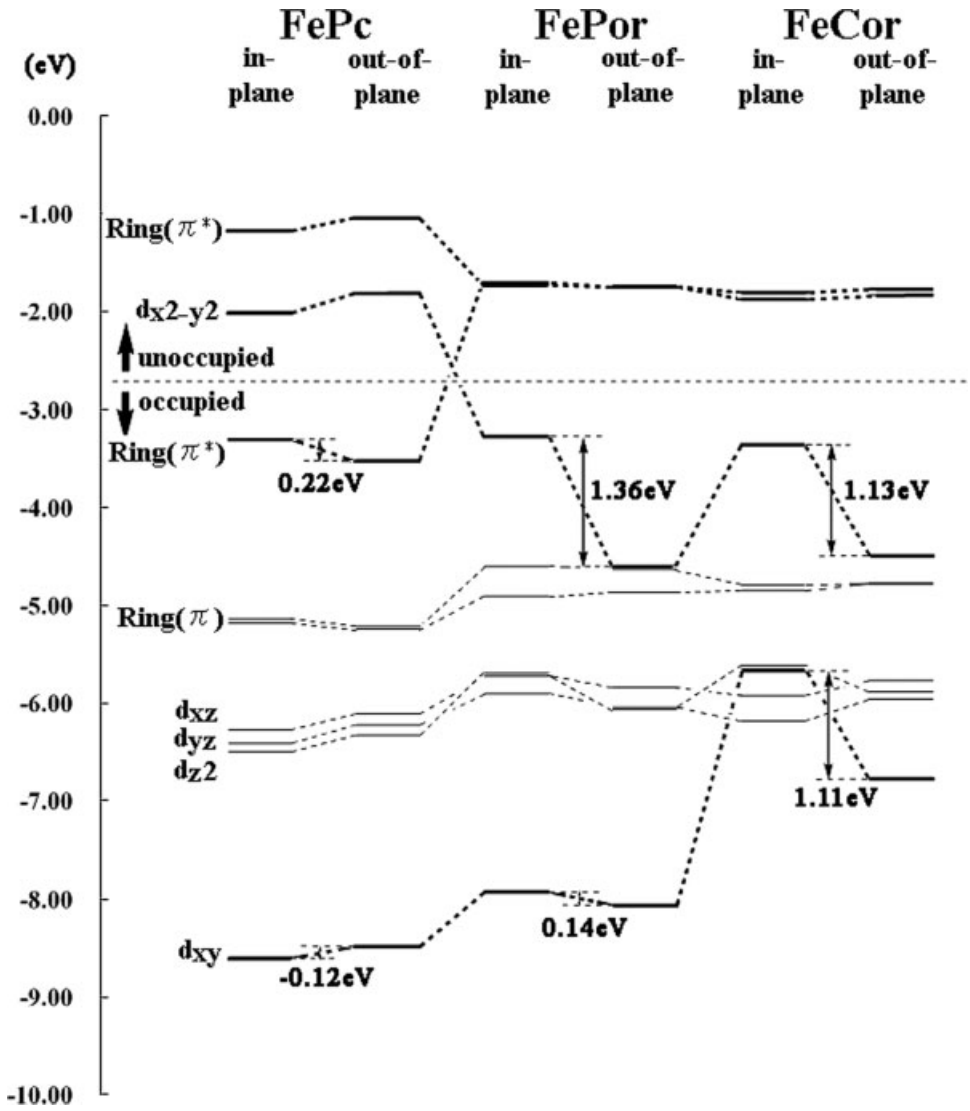

Figure 3. Molecular orbital energy diagram (for SOMOs and alpha spin electrons) of the deoxy complexes in the quintet states. The results for the two structures, in-plane ($d = 0.0$) and out-of-plane, are compared.

atom dislocation was 0.513 Å, which was larger than that of the triplet (0.213 Å) and singlet states (0.224 Å).

On the other hand, the ground state of FePc was calculated to be a triplet state. The quintet and singlet states are 4.70 and 9.97 kcal/mol higher than the triplet state, respectively. Moreover, the Fe atom deviation was not as significant (0.260 Å), which was clearly different from the case of FePor (0.421 Å). The triplet (0.231 Å) and singlet (0.233 Å) states showed similar deviations to the case of FePor, as shown in Table 1.

Among these three complexes, the optimized geometries and stabilities of the quintet states shows characteristic features. To figure out the reason, we analyzed the orbital energy of the complexes in the quintet state as shown in Figure 3. It showed the MO pictures of SOMOs and alpha spin MOs of the unrestricted DFT. In the quintet state, the SOMOs are important: they are the key orbitals $d_x2_{-y}2$ and ring π^*. The orbital shown are characterized as Fe(d-orbital), Ring(π), and Ring(π^*) of porphyrin. The orbital energy in in-plane ($d = 0.0$) and out-of-plane geometries are also compared.

Based on the diagram, the character of the highest singly occupied MO (HSOMO) explains why the Fe atom in FePor and FeCor prefer the out-of-plane position. The HSOMO of FePor and FeCor is the Fe $d_x2_{-y}2$ orbital, while that of FePc is the Ring(π^*) orbital. Because the Fe $d_x2_{-y}2$ orbital has antibonding character with the lone pair of the pyrrole N, the $d_x2_{-y}2$ orbital becomes significantly stable when the Fe atom is in the out-of-plane position. The amount of the stabilization is 1.36 and 1.13 eV for FePor and FeCor, respectively. This would be the reason why the Fe atom stays in the out-of-plane position in the quintet state of FePor and FeCor.

Table 2. The Optimized Structural Parameters and Total Energies of the Oxy-complexes in the Triplet and Singlet States.

	FcPor–O_2		FePc–O_2		FeCor–O_2	
	Triplet	Singlet	Triplet	Singlet	Triplet	Singlet
Relative energy (kcal/mol)	**8.36**	**0.00**	**13.8**	**0.00**	**6.54**	**0.00**
			Optimized geometry			
Distance (Å)						
Fe–Im N	2.14	2.07	2.12	2.08	2.12	2.06
Fe–Pyr N_I	2.09	2.01	1.95	1.95	2.09	2.04
Fe–Pyr N_{II}	2.09	2.03	1.95	1.96	2.10	2.07
Fe–Pyr N_{III}	2.09	2.03	1.95	1.96	2.09	1.97
Fe–Pyr N_{IV}	2.08	2.01	1.95	1.95	2.10	1.96
Fe–O	2.91	1.85	3.01	1.86	2.91	1.84
O–O	1.22	1.29	1.21	1.29	1.21	1.29
Fe–ring plane	**0.394**	**0.0253**	**0.256**	**0.00141**	**0.468**	**0.0326**
Angle (degree)						
Pyr N_I–Fe–Pyr N_{II}	88.8	90.8	94.4	96.9	108.4	104.9
Pyr N_{II}–Fe–Pyr N_{III}	88.9	88.9	84.1	82.8	85.4	87.6
Pyr N_{III}–Fe–Pyr N_{IV}	89.0	90.7	94.5	97.0	74.4	79.0
Pyr N_{IV}–Fe–Pyr N_I	89.0	89.6	84.1	83.2	85.7	88.4
Pyr N_I–Fe–Im N	98.9	89.7	95.7	89.0	99.8	88.5
Pyr N_{II}–Fe–Im N	96.2	89.5	96.2	88.9	97.1	88.5
Pyr N_{III}–Fe–Im N	99.1	89.4	96.7	89.1	101.2	90.6
Pyr N_{IV}–Fe–Im N	97.7	89.5	96.8	89.1	100.0	90.8
Fe–O–O	119.7	118.1	116.6	118.5	118.3	118.4
Dihedral angle (degree)						
Pyr N_I–Fe–Im N–Im C	86.6	135.7	38.0	45.3	103.7	136.6
Pyr N_{II}–Fe–Im N–Im C	−3.15	44.9	−57.1	−51.7	−6.40	31.6
Pyr N_{III}–Fe–Im N–Im C	−93.0	−44.0	−141.9	−134.5	−93.1	−56.0
Pyr N_{IV}–Fe–Im N–Im C	176.8	−134.7	122.7	128.5	−169.0	−135.0

The total energy of the singlet state is taken to be 0.00 kcal/mol for all complexes.

In contrast, the HSOMO of FePc is the Ring(π*) orbital. The Ring(π) and Ring(π*) orbitals originate from the four orbitals of the porphyrin.[52,53] The energy levels of the Ring(π*) orbitals are very close each other in FePor, because of the symmetry. However, in FePc, one of the Ring(π*) orbitals is significantly more stable than the other. This is related to the orbital energy levels of the $C_{20}H_{20}^{2+}$ perimeter model, as clearly explained by a previous study.[54,55] As a result, the lowest quintet state of FePc has an unpaired electron in one of the Ring(π*) orbitals, but not in the Fe $d_{x}2_{-y}2$ orbital. This is also confirmed by Mulliken spin population analysis. In the optimized quintet states, the atomic spin populations of the Fe atom are 3.87 and 3.82 for FePor and FeCor, and in contrast, 2.86 for FePc. This is clearly different from the case of FePor and FeCor. In other words, FePc has a radical in the porphycene ring, and the Fe atom is in the quartet state [Fe(S = 3/2) + Pc(S = 1/2)]. In contrast, FePor and FeCor have Fe(II) ion in the quintet state [Fe(S = 2) + Por(S = 0)]. Therefore, FePc cannot be stable even when Fe atom is in the out of position. The amount of the stabilization is 0.22 eV (1.36 and 1.13 eV for FePor and FeCor, respectively).

Another remarkable orbital is d_{xy} orbital, which is the lowest energy *d*-orbital of Fe atom for FePor and FePc. However, in FeCor, because the ring plane is distorted (symmetry broken), the d_{xy} orbital interacts to the lone pair of the pyrrole N with antibonding character. As a result, this orbital is destabilized in in-plane geometry but stabilized in out-of plane geometry (the same reason for the stabilization of $d_{x}2_{-y}2$ orbital). In contrast, in FePor and FePc, the antibonding interactions vanishes, because the ring planes have high symmetry. The amount of the stabilization is 0.14, −0.12 and 1.11 eV for FePor, FePc, and FeCor, respectively. As a result, the quintet state of FeCor becomes more stable than that of FePor in the out-of-plane geometry.

Ground States of the Oxy-complex: Electronic Structure and Geometry

Next, we investigated the geometry and electronic structures of the ground state of the oxy-complexes. Table2 shows the optimized geometry and the relative energies in each spin multiplicity.

The ground states of the oxy-complex, FePor (Mulliken spin population: Fe: 1.15, O_2: −1.08), FePc (Fe: 1.16, O_2: −1.10), and FeCor (Fe: 1.13, O_2: −1.07), were calculated to be a singlet state. There was no remarkable difference in the optimized geometries among the complexes in the single ground state. The Fe atom located in the in-plane position, and the deviations were calculated to be almost 0.0 Å. The Fe–O_2 and O–O distances

were about 1.85 and 1.29 Å, respectively. The electronic structures of the oxy-complexes in the ground state were also very similar. As shown in the previous article,[44] the Fe d_z2 and the O_2 π^* orbital interacts and compose the σ-bonding orbital. There is no apparent π-bonding orbital. Therefore, the electronic structure of the oxy-complexes is biradical character: spin population in the Fe d_{xz} and the other π^* orbital. Thus, there were no large differences regarding either the optimized geometry or the electronic structure among any of the complexes.

On the other hand, the triplet states located higher than that of the singlet states by 8.36, 13.8, and 6.54 kcal/mol for FePor–O_2, FePc–O_2, and FeCor–O_2, respectively. The Fe–O_2 and O–O distances were very close among the complexes. One characteristic feature was that the Fe atom located out of plane by 0.394, 0.256, and 0.468 Å in FePor−O_2, FePc–O_2, and FeCor–O_2 complexes, respectively. Compared with FePor–O_2 and FeCor–O_2, the out-of-ring deviation was small in FePc–O_2. The amount of the deviation is related to the structure of the deoxy-complexes in its ground state. The out-of-ring deviation was 0.429, 0.231, and 0.513 Å in FePor, FePc, and FeCor complexes, respectively. This is because the electronic structures of the triplet states can be described as the combination of the deoxy-complex and O_2 in their ground states. They are described as Fe(S = 2) + O_2(S = 1) for FePor–O_2 (Mulliken spin population: Fe: 3.88, O_2: −1.99) and FeCor−O_2 (Fe: 3.82, O_2: −1.99) and Fe(S = 1) + O_2(S = 1) for FePc–O_2 (Fe: 2.87, O_2: −1.99). Therefore, from the same discussions as in the deoxy complexes (in the previous section), this explains the reason why the triplet state of FePc–O_2 is unstable compared with those of FePor–O_2 and FeCor–O_2, and why the out-of-ring deviation of the Fe atom is small for FePc–O_2.

The electronic structure of oxyheme (FePor–O_2) has been studied with several theoretical methods but their results were very different to each other, which may indicate that the electronic structure of oxyheme is a rather difficult subject and may include strong electron correlation effects. Recently, elaborate DFT or CASPT2 calculations were performed, and we compare our results with them.[9–14] Siegbahn et al. studied the O_2, CO, and NO bindings to the heme with the histidine residue at the distal site by using the DFT method (B3LYP), although they replaced imidazole of the proximal site with NH_3.[14] Ghosh et al.[9,10] studied the effects of angular changes of the proximal imidazole ring, which can influence the ligand field and binding energies. The electronic structure of the ground state of oxyheme was the same as that of our calculations: open-shell singlet biradical state. The studies using multiconfigurational wave functions were also performed by Kashiwagi et al.[22–24] 10 to 20 years ago with the CASSCF level, in which they suggested that the Hartree–Fock closed-shell configuration Fe(S = 0)+O_2(S = 0) was the main configuration. The SAC/SAC-CI study also suggested the same conclusion.[26] The results of CASSCF calculations strongly depend on the choice of the active space.[56] Ryde et al.[13] studied the ground state of oxyheme with the CASPT2 level at a large active space and large basis set. They suggested the extensive multiconfigurational character of the ground state and a mixture of many different configurations, which were different from the previous CASSCF studies. These results indicate that strong electron correlations may exist in the electronic structures of oxyheme.

The Potential Energy Surfaces for the O_2 Binding Processes

To understand the mechanism of O_2 binding, we studied the potential energy surfaces in the O_2 binding for the singlet and triplet states. Figure 4 shows the potential energy surfaces for the singlet and triplet states. See Figure 2 for the reaction coordinate, d and R.

The Potential Energy Surface for FePor–O_2 and FeCor–O_2 Complex

For FePor–O_2, the details have been described in the previous article.[44] As shown in Figure 4, the potential energy surface of the singlet state is associative over the entire surface. In contrast, the triplet surface is dissociative over the entire area. Because the FePor moiety becomes the quintet ground state in the O_2 dissociation limit, the Fe atom locates in the out-of-plane position. The potential surface clearly shows that the O_2 binding requires the intersystem crossing from triplet to singlet state. The crossing region would be around d = 0.2–0.3 Å, R = 2.2–2.5 Å. The O_2 binding process should include the intersystem crossing region to reach the singlet O_2 binding state.

The O_2 binding potential surface for the FeCor–O_2 complex resembles that for FePor–O_2. The ground state is singlet in the O_2 binding state and changes into triplet state in the dissociation limit. There is intersystem-crossing region around d = 0.1–0.2 Å and R = 2.1–2.5 Å. Therefore, the O_2 binding process would be very similar to that of FePor–O_2.

The Potential Energy Surface for FePc–O_2 Complex

Next, we explain the potential energy surface of the porphycenes complex. As seen in Figure 4, the potential energy surface of the singlet state is associative, and that of the triplet state is dissociative. This is the same feature generally seen in the porphyrin isomer complex. However, the important difference in the Pc case is that the singlet state is more stable than the triplet state in the dissociation limit. This is because the ground state of the deoxy complex is triplet, not quintet as the case of porphyrin and corrphycene as described earlier. The FePc + O_2 system is singlet [Fe(S = 1) + O_2(S = 1)] in the O_2 dissociation limit. The FePc–O_2 complex is also singlet after the O_2 binding, as described above. Therefore, the O_2 binding process does not require intersystem crossing. In this sense, the mechanism of O_2 binding in the FePc–O_2 complex is fundamentally different from that in the FePor–O_2 and FeCor–O_2 complexes.

The O_2 Binding Mechanism

As shown in Figure 5, we extracted the energy-minimum pathway along the O_2 binding process from the potential surface. For FePor–O_2, the details have been reported in the previous article.[44] In the O_2 binding process, the complex reaches the intersystem crossing point on the triplet potential energy surface after climbing the energy barrier of 3.0 kcal/mol. The spin multiplicity changes into the singlet state, and Fe–O_2 bond is formed. The overall reaction energy is 8.4 kcal/mol. In the O_2 dissocia-

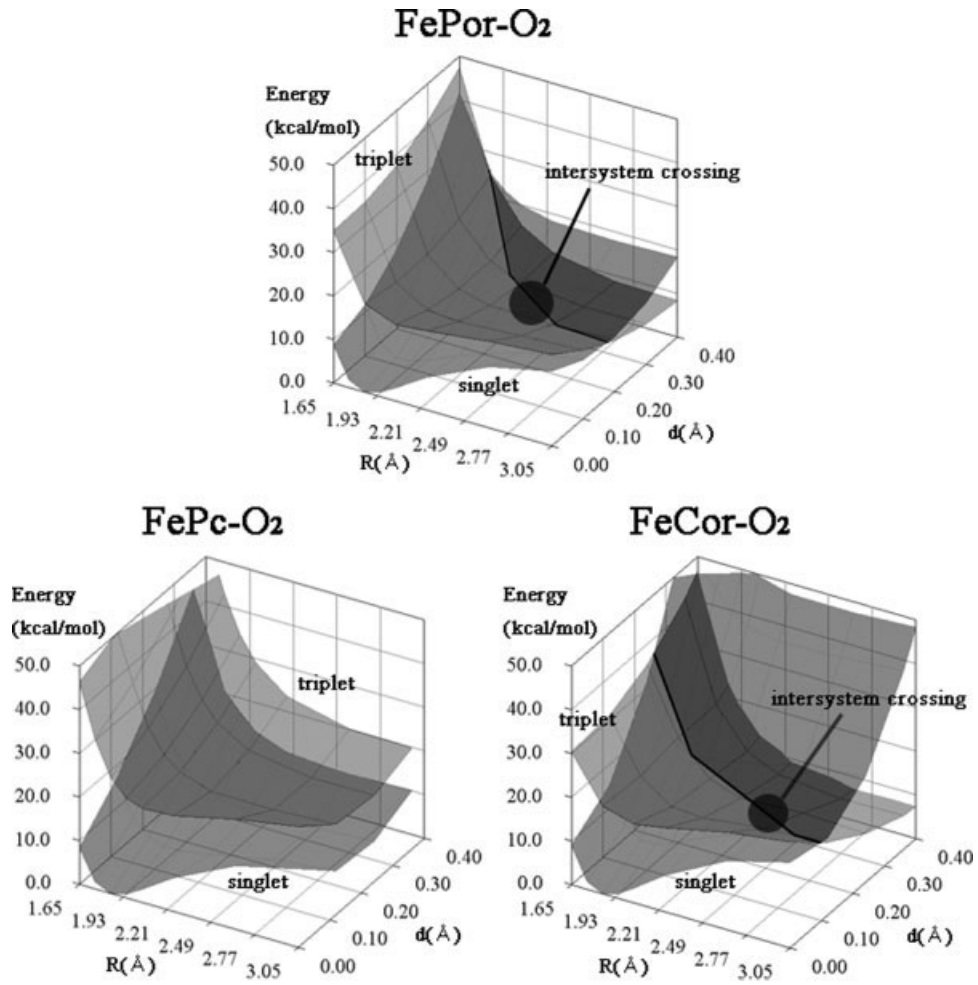

Figure 4. The potential energy surfaces of FePor–O_2, FePc–O_2, and FeCor–O_2 in the lowest singlet and triplet states. The intersystem crossing could occur around $d = 0.2$–0.3 Å and $R = 2.2$–2.5 Å in FePor–O_2 and around $d = 0.1$–0.2 Å and $R = 2.1$–2.5 Å in FeCor–O_2. There is no intersystem crossing region in the FePc–O_2 potential surface.

tion process, the system needs 11.4 kcal/mol to reach the intersystem crossing point.

The potential curve of the FeCor–O_2 as shown in Figure 5 is very similar to that of FePor–O_2. The activation energy for the O_2 binding is 6.5 kcal/mol, and the reaction energy is 6.5 kcal/mol as binding energy. In the O_2 dissociation, the energy barrier is calculated to be 13.0 kcal/mol.

In contrast, FePc–O_2 complex only uses the singlet surface for the O_2 binding/dissociation without spin conversion. The binding energy is 10.7 kcal/mol. The O_2 binding process has no energy barrier. We note that our calculations included only the O_2–Fe–Porphycene–Imidazole and the O_2 binding would be barrierless within the complex. In the actual system, the pathway to the heme might include some energy barrier due to van der waals interactions between O_2 and the protein residues.

The O_2 binding energy of the FePc–O_2 complex is the largest, and that of FeCor–O_2 is the smallest of the three porphyrin isomers. This tendency qualitatively explains the experimental fact that the FePc reconstituted heme exhibits very high O_2 binding affinity[36,37] and the FeCor one shows only small O_2 binding affinity.[38,39]

On the Equilibrium Constant of O_2 Binding

Using the calculated potential surfaces, we estimated the equilibrium constant for the O_2 binding in each complex and compared with the experimental results observed in human myoglobin and its reconstituted ones.

$$K = e^{-\frac{\Delta G}{RT}} \approx e^{-\frac{\Delta E}{RT}}. \quad (2)$$

In eq. (2), we assumed that the entropy effects were constant and used the binding energy (ΔE) instead of free energy (ΔG). The theoretically estimated equilibrium constants obtained from eq. (2) and the experimental values[36–39] are compared in Table3. The

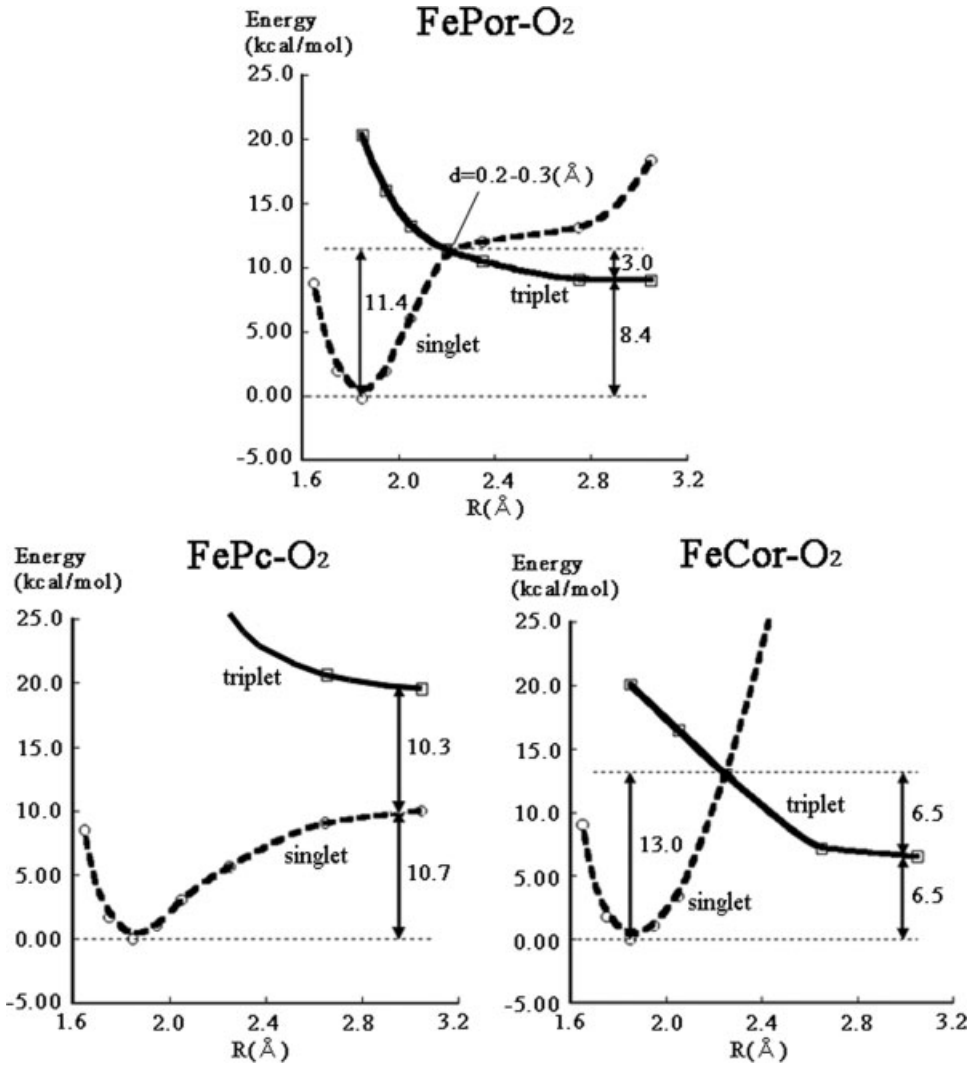

Figure 5. Potential curves for the O_2 binding along the energy minimum pathway. The solid line (---) and dashed line (- - - -) denote the triplet and singlet states, respectively.

theoretically estimated value of FePor–O_2 reported previously[44] was very close to the experimental value. For FePc–O_2, the present estimation was around 50 times larger than that for FePor–O_2. The experimental value was around 1000 times larger than natural myoglobin including FePor–O_2. Our estimation shows the same tendency observed in the experiment, which indicates that the FePc–O_2 moiety of the heme explains the large portion of the high O_2 affinity in the reconstituted myoglobin.[36,37] For FeCor–O_2, the theoretical and experimental values were also very close to each other. The theoretical estimation reproduced the small O_2 affinity observed by the experiment.[38,39]

The present estimations for the equilibrium constant reasonably agrees to the trend observed in the experiments for three isomers.[36–39] Although we did not consider the effects of the surrounding proteins and the entropy, the present results could be a reasonable basis for explaining the experimental findings.[36–39]

Table 3. Equilibrium Constants Estimated by the Reaction Energy.

K [M^{-1}]	Theoretical estimation	Experimental value
FePor	1.8×10^6 (20°C)	1.1×10^6 (20°C)
FePc	7.0×10^7 (25°C)	1.1×10^9 (25°C)
FeCor	7.0×10^4 (20°C)	1.5×10^4 (20°C)

The experimental values are also shown for the comparison.

Conclusion

There are several porphyrin isomers: porphycene and corrphycene. They were used for the alternative to the porphyrin in myoglobin. Such reconstituted myoglobins show singular O_2 affinity, which is quite different from the native myoglobin. We

theoretically investigated the mechanism of O_2 binding to FePor, FePc, and FeCor complexes using the Density Functional Theory calculations.

First, the ground state of the deoxy and oxy complexes were determined. In deoxy complexes, the ground states of both FePor and FeCor are quintet states, and the Fe atom significantly deviates from the ring plane. In contrast, the ground state of FePc is a triplet state, and the Fe atom shows moderate deviation from the ring plane. In the quintet states, the $d_x2_{-y}2$ orbital (SOMO) is stabilized when the Fe atom locates the out-of-plane positions. This is because the $d_x2_{-y}2$ orbital has antibonding character between the Fe $d_x2_{-y}2$ and the porphyrin π orbitals. However, the $d_x2_{--y}2$ orbital is not occupied in the quintet state of FePc. Instead, the porphycene's Ring(π^*) orbital becomes SOMO. Therefore, the quintet state of FePc is not stabilized as those of FePor and FeCor. This is the electronic-structural origin of the high O_2 affinity in the porphycenes reconstituted myoglobin. In the oxy complexes, the ground states were calculated to be the singlet states for all complexes, and the Fe atom locates in-plane position. There are no large differences in the optimized geometries and the electronic structures among the isomers. The electronic structures of the triplet states are Fe($S = 2$) + O_2($S = 1$), and the Fe–Ring–Im moieties are very close to that of the quintet states in deoxy complexes.

Next, we investigated the potential energy surfaces for the O_2 binding. In all complexes, the potential energy surfaces of the singlet state are associative, while they are dissociative for the triplet states. For FePor–O_2 and FeCor–O_2, there is the intersystem crossing regions between the singlet and triplet states. This area is also the transition state in the O_2 binding pathway. Therefore, the O_2 binding process for both FePor–O_2 and FeCor–O_2 includes the intersystem crossing. In contrast, for FePc–O_2, the triplet state is more unstable than the singlet state, and there is no crossing between the two surfaces. Therefore, the O_2 binding of the FePc–O_2 complex proceeds only on the singlet surface. There is no energy barrier in the O_2 binding. These potential surfaces qualitatively explain the O_2 affinity observed in the experiments.

We discussed the O_2 affinities by estimating the equilibrium constant. The theoretical estimation reproduced the trend of the experimental equilibrium constant. This result also indicate that the potential energy surface reasonably explains the major part of the O_2 affinities, FePc–O_2 > FePor–O_2 > FeCor–O_2, observed in the experiments.

Acknowledgments

A part of the computations was performed in the Research Center for Computational Science, Okazaki, Japan.

References

1. Bernal, J. D.; Fankuchen, I.; Perutz, M. F. Nature 1938, 141, 523.
2. Monod, J.; Wyman, J.; Changeux, J. P. J Mol Biol 1965, 12, 88.
3. Englander, J. J.; Rumbley, J. N.; Englander, S. W. J Mol Biol 1998, 284, 1707.
4. Bettati, S.; Mozzarelli A.; Perutz, M. F. J Mol Biol 1998, 281, 581.
5. Kim, H. W.; Shen, T. J.; Ho, N. T.; Zou, M.; Tam, M. F.; Ho, C. Biochemistry 1996, 35, 6620.
6. Tokita, Y.; Nakatsuji, H. J Phys Chem B 1997, 101, 3281.
7. Jewsbury, P.; Yamamoto, S.; Minato, T.; Saito, M.; Kitagawa, T. J Phys Chem 1995, 99, 12677.
8. Obara, S.; Kashiwagi, H. J Chem Phys 1982, 77, 3155.
9. Ghosh, A.; Bocian, D. F. J Phys Chem 1996, 100, 6363.
10. Ghosh., A.; Wondimagegn, T. J Am Chem Soc 2000, 122, 8101.
11. Schenk, G.; Pau, M. Y. M.; Solomon, E. I. J Am Chem Soc 2004, 126, 505.
12. Angelis, F. D.; Jarzecki, A. A.; Car, R.; Spiro, T. G. J Phys B 2005, 109, 3065.
13. Jensen, K. P.; Roos, B. O.; Ryde, U. J Inorg Chem 2005, 99, 45.
14. Blomberg, L. M.; Blomberg, M. R. A., Siegbahn, P. E. M. J Inorg Chem 2005, 99, 949.
15. Taranto, A. G.; Carneiro, J. W. M.; Oliveira, F. G. J Mol Struct (Theochem) 2001, 539, 267.
16. Marechal, J.; Barea, G.; Maseras, F.; Lledos, A.; Mouawad, L.; Perahia, D. J Comput Chem 2000, 21, 282.
17. Maseras, F. New J Chem 1998, 22, 327.
18. Barea, G.; Maseras, F.; Lledos, A. Int J Quantum Chem 2001, 85, 100.
19. Rovira, C.; Kunc, K.; Hutter, J.; Ballone, P.; Parrinello, M. Int J Quantum Chem 1998, 69, 31.
20. Rovira, C.; Parrinello, M. Int J Quantum Chem 1998, 70, 387.
21. Rovira, C.; Parrinello, M. Int J Quantum Chem 2000, 80, 1172.
22. Choe, Y.; Hashimoto, T.; Nakano, H.; Hirao, K. Chem Phys Lett 1998, 295, 380.
23. Yamamoto, S.; Kashiwagi, H. Chem Phys Lett 1989, 161, 85.
24. Yamamoto, S.; Kashiwagi, H. Chem Phys Lett 1993, 205, 306.
25. Choe, Y.; Nakajima, T.; Hirao, K.; Lindh, R. J Chem Phys 1999, 111, 3837.
26. Nakatsuji, H.; Hasegawa, J.; Ueda, H.; Hada, M. Chem Phys Lett 1996, 250, 379.
27. Jewsbury, P.; Yamamoto, S.; Minato, T.; Saito, M.; Kitagawa, T. J Am Chem Soc 1994, 116, 11586.
28. Springer, B. A.; Sligar, S. G.; Olson, J. S.; Phillips, G. N., Jr. Chem Rev 1994, 94, 699.
29. Allocatellli, C. T.; Cutruzzola, F.; Brancaccio, A.; Vallone, B.; Brunori, M. FEBS Lett 1994, 352, 63.
30. Turano, P.; Lu, Y. In Handbook on Metalloproteins; Sigel, S.; Sigel, H., Eds.; Marcel Dekker: New York, 2001, p. 269.
31. Raven, E. L.; Mauk, A. G. In Advances in Inorganic Chemistry; Sykes, A. G.; Mauk G., Eds.; Academic Press: San Diego, 2001, p. 1, vol. 51.
32. Ozaki, S.; Roach, M. P.; Watanabe Y. Acc Chem Res 2001, 34, 818.
33. Neya, S.; Kaku, T.; Funasaki, N.; Shiro, Y.; Iizuka, T.; Imai, K.; Hori, H. J Biol Chem 1995, 270, 13118.
34. Neya, S.; Hori, H.; Imai, K.; Kawamura–Konishi, Y.; Suzuki, H.; Shiro, Y.; Iizuka, T.; Funasaki, N. J Biochem 1997, 121, 654.
35. Fitzgerald, J. P.; Haggerty, B. S.; Rheingold, A. L.; May, L.; Brewer, G. A. Inorg Chem 1992, 31, 2006.
36. Hayashi, T.; Dejima, H.; Matsuo, T.; Sato, H.; Murata, D.; Hisaeda, Y. J Am Chem Soc 2002, 124, 11226.
37. Matsuo, T.; Dejima, H.; Hirota, S.; Murata, D.; Sato, H.; Ikegami, T.; Hori, H.; Hisaeda, Y.; Hayashi, T. J Am Chem Soc 2004, 126, 16007.
38. Neya, S.; Tsubaki, M.; Hori, H.; Yonetani, T.; Funasaki, N. Inorg Chem 2001, 40, 1220.
39. Neya, S.; Funasaki, N.; Hori, H.; Imai, K.; Nagatomo, S.; Iwase, T.; Yonetani, T. Chem Lett 1999, 28, 989.
40. Hayashi, T.; Hisaeda, Y. Acc Chem Res 2002, 35, 35.
41. Heleg–Shabtai, V.; Gabriel, T.; Willner, I. J Am Chem Soc 1999, 121, 3220.

42. Christopher, F., Jr.; Takimura, T.; Sessler, J. L. Abstracts of Papers 213th ACS National Meeting San Francisco, CA; American Chemical Society: Washington, DC, 1997, INOR-519.
43. Sotiriou–Leventis, C.; Chang, C. K. Inorg Chim Acta 2000, 311, 113.
44. Nakashima, H.; Hasegawa, J.; Nakatsuji, H. J Comp Chem, to appear.
45. Frisch, M. J.; Trucks, G. W.; Schlegel, H. B.; Scuseria, G. E.; Robb, M. A.; Cheeseman, J. R.; Strain, M. C.; Burant, J. C.; Stratmann, R. E.; Dapprich, S.; Kudin, K. N.; Millam, J. M.; Daniels, A. D.; Petersson, G. A.; Montgomery, J. A.; Zakrzewski, V. G.; Raghavachari, K.; Ayala, P. Y.; Cui, Q.; Morokuma, K.; Foresman, J. B.; Cioslowski, J.; Ortiz, J. V.; Barone, V.; Stefanov, B. B.; Liu, G.; Liashenko, A.; Piskorz, P.; Chen, W.; Wong, M. W.; Andres, J. L.; Replogle, E. S.; Gomperts, R.; Martin, R. L.; Fox, D. J.; Keith, T.; AlLaham, M. A.; Nanayakkara, A.; Challacombe, M.; Peng, C. Y.; Stewart, J. P.; Gonzalez, C.; Head–Gordon, M.; Gill, P. M. W.; Johnson, B. G.; Pople, J. A. Gaussian98; Gaussian Inc.: Pittsburgh, PA, 1998.
46. Hariharan, P. C.; Pople, J. A. Theor Chim Acta 1973, 28, 213.
47. Phillips, S. E. V. Nature 1978, 273, 247.
48. Phillips, S. E. V. J Mol Biol 1980, 142, 531.
49. Fermi, G. J Mol Biol 1975, 97, 237.
50. Momenteau, M.; Scheidt, W. R.; Eigenbrot, C. W.; Reed, C. A. J Am Chem Soc 1988, 110, 1207.
51. Jameson, G. M.; Rodley, G. A.; Robinson, W. T.; Gagne, R. R.; Reed, C. A., Collman, J. P. Inorg Chem 1978, 17, 850.
52. Gouterman, M. The Porphyrins; Academic Press: New York, 1978, p. 1.
53. Gouterman, M. J Mol Spectrosc 1961, 6, 138.
54. Waluk, J.; Müller, M.; Swiderek, P.; Köcher, M.; Vogel, E.; Hohlneicher, G.; Michl, J. J Am Chem Soc 1991, 113, 5511.
55. Waluk, J.; Michl, J. J Org Chem 1991, 56, 2729.
56. Pierloot, K. Mol Phys 2003, 101, 2083.